International Journal on Magnetic Particle Imaging
Vol 12, No 1, Suppl 1, Article ID 2603017, 3 Pages

Proceedings Article

The multi-color relaxation wall: fundamental limits of spectral separation in physics-based MPI

Seungjun Oh[a] · Hafiz Ashfaq Ahmad[a] · Muhammad Umar Tahir[a] · Jungwon Yoon[a,*]

[a]AI Convergence Department, Gwangju Institute of Science and Technology, Gwangju, Republic of Korea
*Corresponding author, email: jyoon@gist.ac.kr

Abstract

Multi-color Magnetic Particle Imaging (mcMPI) differentiates biological processes by exploiting particle-specific relaxation times, but conventional approaches rely on extensive calibration that limits practical deployment. Also, quantitative approaches linking relaxation time ratios to separability of multiple particles remain underexplored. Here, we use spectral separability derived from the frequency-domain correlation and examine how relaxation-induced frequency attenuation constrains spectral separability in mcMPI through a physics-based computational forward model with particle-specific Debye operators, enabling calibration-free multi-color reconstruction. Simulations demonstrate that, at a representative relaxation time ratio, spectral separability can be quantified and leads to feasible multi-color image reconstruction, while signals from long-relaxation particles are attenuated.

I. Introduction

Multi-color MPI (mcMPI) visualizes multiple SPION populations via relaxation-dependent spectral responses [1, 2]. Previous studies demonstrated multi-color separation using both system-matrix-based and calibration-free approaches[3, 4], but quantitative metrics linking relaxation-time ratios to separability remain underexplored. Physics-based frameworks [5] overcome calibration and enable frequency-domain analysis, but typically employ a single global delay that cannot encode particle-specific relaxation.

Tay et al. [6] identified the “relaxation wall,” where particles with $\omega\tau \gg 1$ undergo frequency-dependent attenuation that reduces detectability. In mcMPI, high relaxation time ratio (τ-ratio) values enable spectral separation while long-τ particles exhibit reduced SNR.

The present work quantifies separability by formulating spectral separability as a frequency-domain consequence of relaxation-induced attenuation. Furthermore, this framework reconstructs multi-color images at a representative τ-ratio.

II. Methods

Under the adiabatic assumption, the physics-based forward model [5] describes the MPI signal as $\bar{s}_0 = \mathbf{V}EH\rho$, where H models the MPI PSF, E performs FFP sampling, and $\mathbf{V}$ applies FFP velocity weighting. The receive chain gives $\bar{s} = \Gamma\bar{s}_0$. For multi-color imaging, particle-specific Debye modulation is incorporated into the H term as

$$H_j(\omega) = H(\omega)D_j(\omega), \quad D_j(\omega) = \frac{1}{1 + i\omega\tau_j}. \tag{1}$$

The index j denotes each particle population.

Spectral separability is quantified using a normalized metric S, derived from the frequency-domain correlation between particle-specific relaxation responses,

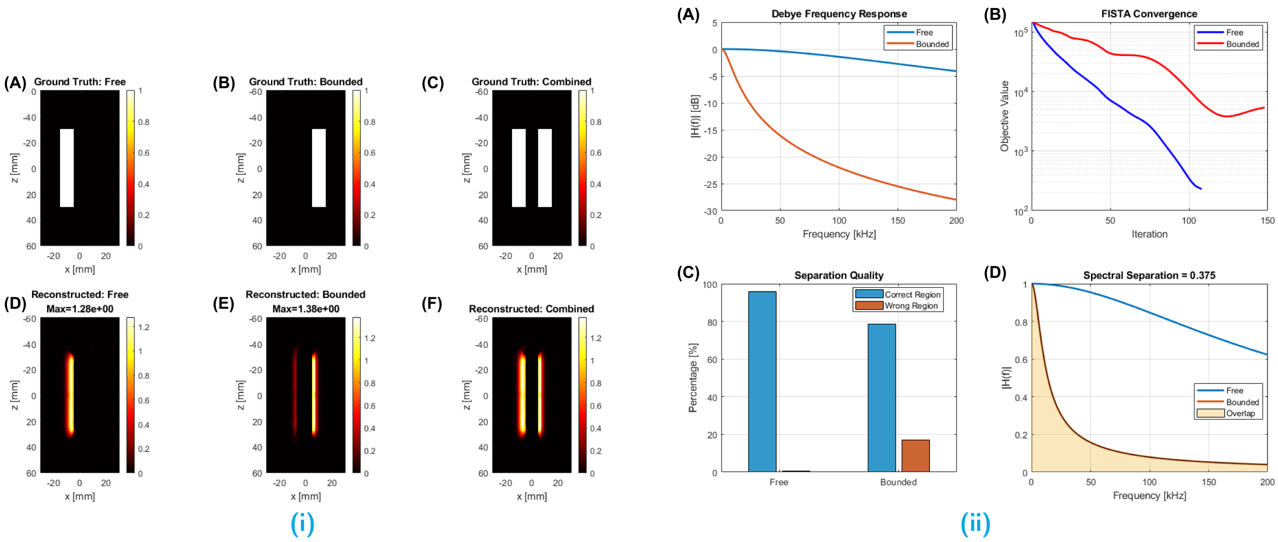

Figure 1: Overview of physics-based multi-color reconstruction and spectral analysis at a $20\times\tau$-ratio. Subfigure (i) shows the multi-color reconstruction results of each particle population, and subfigure (ii) presents a quantitative spectral analysis illustrating relaxation-induced separability with a corresponding spectral metric of $S \approx 0.38$ at $f_{\text{drive}} = 45$ kHz.

where larger S indicates reduced spectral overlap. Because the scanning trajectory is identical for all particles, $\bar{s} = \Gamma \mathbf{V} E\left(\sum_j H_j \rho_j\right)$. We reconstruct by

$$\min_{\rho_j \geq 0} \left\| \bar{s} - \sum_j A_j \rho_j \right\|_2^2 + \sum_j \lambda_j \|\nabla \rho_j\|_2^2, \quad A_j = \Gamma \mathbf{V} E H_j, \quad (2)$$

with Debye-aware regularization scaling $\lambda_j = \lambda_0 / |D_j(f_{\text{drive}})|$ to account for relaxation-induced attenuation from the drive frequency (f_{drive}).

Simulations use Momentum parameters (5.7 T/m, 45 kHz, 20/23 mT) [7, 8] and two particle populations (τ_1=1 μs, τ_2=20 μs), chosen to represent free-circulating (τ_1) and tissue-bound (τ_2) particle states, respectively.

III. Results and Discussion

Figure 1(i) shows multi-color reconstruction images, demonstrating successful separation of the two particle populations. The extracted Debye responses are consistent with the relaxation times τ_1 and τ_2(Figure 1(ii)). At 45 kHz, the amplitude ratio $|D_1|/|D_2| \approx 5.7$ (~15 dB difference) indicates the multi-color extension of the relaxation wall: increasing τ-ratio improves separability while attenuating long-τ particle signals. Frequency-domain correlation reflects partial spectral overlap between particle responses, with a corresponding spectral separability of $S \approx 0.38$. The proposed formulation was numerically consistent under the investigated relaxation contrast. The multi-color relaxation trade-off is quantified: increasing relaxation-time contrast improves spectral separability while attenuating long-τ particle signals, indicating an inherent constraint on achievable multi-color image quality. For the 45 kHz drive frequency, τ-ratios near 20× yielded sufficient separability ($S \approx 0.38$) while maintaining detectable signal levels for both populations, suggesting a practical operating regime for particle selection.

IV. Conclusion

We quantified spectral separability and reconstructed multi-color images using particle-specific Debye operators within a physics-based framework. Simulations demonstrate effective multi-color separation for particles with distinct relaxation times. Our results highlight that practical multi-color image quality is governed by the interplay between particle relaxation times. Future systematic parameter sweeps can further delineate practical operating regimes and extend toward viscosity-dependent functional imaging.

Acknowledgments

This work was supported by the NRF of Korea grant funded by the MSIT (No. RS-2025-00554248).

Author's statement

Conflict of interest: Authors state no conflict of interest. This research did not involve human subjects or animal experiments.

References

[1] C. Stehning, B. Gleich, and J. Rahmer. Simultaneous magnetic particle imaging (mpi) and temperature mapping using multi-color mpi. *International Journal on Magnetic Particle Imaging*, 2(2):1602002, 2016, doi:10.18416/IJMPI.2016.1602002.

[2] B. Gleich and J. Weizenecker. Tomographic imaging using the nonlinear response of magnetic particles. *Nature*, 435(7046):1214–1217, 2005, doi:10.1038/nature03808.

[3] J. Rahmer, A. Halkola, B. Gleich, I. Schmale, and J. Borgert. First experimental evidence of the feasibility of multi-color magnetic particle imaging. *Physics in Medicine and Biology*, 60(5):1775–1791, 2015, doi:10.1088/0031-9155/60/5/1775.

[4] Y. Muslu, M. Utkur, O. B. Demirel, and E. U. Saritas. Calibration-free relaxation-based multi-color magnetic particle imaging. *IEEE Transactions on Medical Imaging*, 37(8):1920–1931, 2018, doi:10.1109/TMI.2018.2810278.

[5] T. Sanders, J. Konkle, O. C. Sehl, A. R. Mohtasebzadeh, J. M. Greve, and P. W. Goodwill. A physics-based computational forward model for efficient image reconstruction in magnetic particle imaging. *IEEE Transactions on Medical Imaging*, 44(5):2319–2329, 2025, doi:10.1109/TMI.2025.3530316.

[6] Z. W. Tay, D. W. Hensley, E. C. Vreeland, B. Zheng, and S. M. Conolly. The relaxation wall: Experimental limits to improving MPI spatial resolution by increasing nanoparticle core size. *Biomedical Physics & Engineering Express*, 3(3):035003, 2017, doi:10.1088/2057-1976/aa6ab6.

[7] Magnetic Insight, Inc., Momentum™ preclinical magnetic particle imaging system, `https://www.magneticinsight.com/momentum/`, 2024.

[8] O. C. Sehl, K. Guo, A. R. Mohtasebzadeh, P. Kim, B. Fellows, M. Weyhmiller, P. W. Goodwill, M. Wintermark, S. Y. Lai, P. J. Foster, and J. M. Greve. Magnetic particle imaging enables nonradioactive quantitative sentinel lymph node identification: Feasibility proof in murine models. *Radiology Advances*, 1(3):umae024, 2024, doi:10.1093/radadv/umae024.

